International Journal of Computer Information Systems and Industrial Management Applications
ISSN 2150-7988 Volume 18(3s) 2026 pp. 219-234
https://doi.org/10.70917/ijcisim-2026-2324
Article

A Fuzzy Logic-Based On-Demand Charging Algorithm for Wireless Rechargeable Sensor Networks with Several Chargers

Kumar Dayanand[1], Udai Shankar[2], Mohit Kumar[3]

[1,2]Department of Computer Engineering & Applications, IET, Mangalayatan University, Beswan, Aligarh,
[3]MIT Art, Design and Technology University, Rajbaug, Pune
[1]20220934_dayanand@mangalayatan.edu.in, 2udai.shankar@mangalayatan.edu.in, 3mohitsmailbox13@gmail.com

Abstract: The adoption of "Wireless Rechargeable Sensor Networks" (WRSNs) has been substantially aided by mobile chargers. The majority of current research has been on charging the WRSNs on-demand, but few concentrations has made to jointly taking into account "Multiple Mobile Chargers" (MCs) and multi-node energy transfer to decide when to charge energy-hungry nodes. Additionally, the majority of scheduling plans fail to take into account a variety of network characteristics while making decisions, and ignore the problem of charging nodes with unequal energy consumption rates at the wrong time. This work addresses the aforementioned concerns together in this study and provide a unique scheduling strategy for on-demand charging in WRSNs. To distribute the MCs and evenly distribute their burden across the network, first introduce an effective network partitioning approach. This work uses fuzzy logic to combine different network parameters to determine the MCs' charge schedule. In addition, an equation is developed in this study to determine the charging threshold for nodes with variable rates of energy consumption. Numerous simulations are run to demonstrate the usefulness and efficiency of our method. According to several performance criteria such as average charging latency, survival rate, moving speed time, saturation time, simulation time and energy use efficiency. The proposed Determination of Charging Schedule Request using Fuzzy Logic (DCSR-FL) algorithm has achieve 34%, 98%, 97%, 0.12% and 0.29 (hours) average charging latency, survival rate, energy, saturation rate, and moving speed respectively. The comparative findings show that the suggested scheme outperforms as 0.34 (hour) state-of-the-art methods in terms of charging performance. The suggested method performs better than uneven cluster-based mobile charging (UCMC) and on-demand multi-node charging based on traveling salesman problem (OMC_TSP).

Keywords: Wireless rechargeable sensor networks, Fuzzy logic, On-demand, Mobile charger, Charging schedule.

1. INTRODUCTION

The "Wireless Rechargeable Sensor Networks" (WRSNs) monitor the characteristics and records of a target machines with hundreds of different heterogeneous and homogenous sensor nodes for random throughout of geographic area [1, 2]. With low energy, processing, sensing, and wireless communication resources, ubiquitous nodes can process data (such as compression, aggregation, or fusion) and transport it to the preservation. This can also sense information (such as temperature or humidity). Disaster warning [3], environmental monitoring [4], military surveillance [5], explosion prevention [6], and aviation [7] are a few possible uses for WRSNs.

Some authors have suggested "clustering algorithms" [8] and "Routing Protocol" [9] to improve resource efficiency because to the limited power supplies of nodes. However, the historically restrictive power supply has evolved into the WRSNs' bottleneck, which limits the network longevity. Other researchers have suggested several methods for capturing natural energy, such as wind [10], solar, vibration [11-12] to increase the lifespan. Because it is also susceptible to environmental conditions, these systems cannot deliver consistent energy supplies. To solve the energy issues in WRSNs, "Wireless Power Transfer" (WPT) technology has recently been created. "Wireless Rechargeable Sensor Networks (WRSNs)" are this kind of network. [13]. Wireless charging vehicles (WCVs) are the

energy suppliers in WRSNs, which move through the network and charge the sensor nodes. Wireless charging provides a dependable and manageable energy source for WRSNs. WRSNs have an efficient energy source, but also confront many more difficulties than conventional WSNs. First, because sensors perform diverse activities, they require different rates of energy utilisation. Before any sensors run out of power, WCVs must quickly refuel them in order to maintain ongoing network operation [14]. A single WCV with a constrained energy capacity is unable to fully recharge all of the sensors in large-scale WRSNs, which is the second problem. Several WCVs must operate simultaneously in WRSNs to achieve eternal operation [15, 16]. However, the cost of WRSNs deployment is significantly impacted by the quantity of WCVs. Only the necessary amount of WCVs is required to serve all asking nodes in order to increase WRSNs efficiency. The charge scheduling technique is therefore an existing problem [16–18].

To tackle the concerns mentioned earlier, this work proposes the "Instant On-demand Charging Strategy (IOCS)", which makes use of presence of numerous WCVs as well as enables it to choose the best options on the basis of a common measure of temporal-, spatial-, and sensory-event needs from charging requests. The specific contributions to this undertaking are as follows.

- The temporal and geographical characteristics of the charging demand as well as the activities that nodes have completed are connected to various crucial parameters in the charging requirements of sensors. The proposed IOCS uses the unified charging priority to establish charging sequences by combining these parameters into a single united metric. As far as has aware, this is the first paper to suggest this one crucial criterion for charging priority.
- After carefully examining and researching the operation of sensors in WRSNs, an enhanced K-means method utilizing node positions and energy usage rates is presented to categorise service sub-queues. Each charging request node is divided into a different sub-queue. Depending on the battery capacity, each WCV answers to a single sub-queue.
- IOCS beats other state-of-the-art approaches greatly, according to extensive simulations that were run to compare it to them.

The remainder of this essay is organised as follows: In Section 2, there is a list of works. The model of the preliminary system is shown in Section 3. Section 5 demonstrates the suggested methodology's thorough formulation. The outcome of the simulation is displayed in Section 6. Section 5 wraps up the essay has also made recommendations for further research.

2. RELATED WORK

A lot of study has been done on the usage of WCVs in WRSNs to increase network longevity. The main areas of study were improving WCV charging effectiveness and WRSN sensor maintenance. According to these studies, there are two categories of charging job scheduling methods for WRSNs: predefined charging strategies and real-time charging strategies. The majority of past studies on WRSNs have used predetermined charging techniques, which means that each WCV follows a static charging path and has a set charging timetable. The WCV travels via nodes and distributes energy in accordance with the planned charging schedule.

Typically, the demanding or charging strategy relies on model of the nodes' power absorption and distribution results in a Travelling Salesman Problem (TSP). The best route for WCVs to take is designed using a Hamiltonian cycle. In TSP, ant colony algorithm (ACO) is frequently employed [19]. It uses distributed computing, which has powerful global search capabilities and yields helpful information feedback. The two main predetermining charging techniques are single-node and multi-node charging schemes. [20] Suggested a path scheduling technique depending upon the sensor nodes' and also address the issue of energy efficiency. [21] Presented a predefined charge method based on lifetime forecasting. A pricing system based on the variation of the nodes' remaining lifetime was investigated by certain researchers [22]. The dual-node charging strategy is a better way to charge numerous nearby nodes at once. The result of charging numerous nodes was a significant increase in charging efficiency. The anticipated status of the node and remaining energy are emphasised by predetermined charging strategies. However, the dynamic variation in the node's energy consumption rate in WRSNs [23] is caused by the intricate environmental changes. As a result, the predefined charging technique has a far higher computational cost.

Real-time pricing techniques may be utilised to mitigate the effect of unpredictability problems in WRSNs, according to one suggestion. When using the dynamic charging approach, the node initiates a charging request when its remaining energy falls below a certain level [24]. The asking sensor is promptly recharged by the WCV in

accordance with the accusing plan based on some pre-established rules. In accordance with their arrival time, billing requests are fulfilled. In [25] the "First Come First Served (FCFS)" technique ignores spatial considerations in favour of determining the charge schedule based on temporal priorities. The NJNP technique, or nearest job next with pre-emption, was disclosed in [26]. Similar distinctions can be made between single-WCV charging techniques and multi-WCV collaborative charging strategies when describing real-time charging strategies. To improve scheduling performance, a pricing system that combines arrival time and distance was suggested [27]. The authors in [28] looked at the charging method that combines distance to WCV, residual energy, and critical node density. One WCV cannot feed all the sensors in large-scale WRSNs, which may include thousands of nodes. In light of this, some authors suggested dual WCV charging schemes. The authors described a multi-WCV charging strategy based on evolutionary algorithms with temporal sliding windows in [29]. To solve the cooperative charging issue of several WCVs, Lin et al. [30] created a cooperative charging model and demonstrated the existence of a Nash equilibrium point. The majority of charging strategies in use today merely take into accounts the sensor's location, stochastic charging request, and residual energy when determining the charging order. These variables interact with one another and are complex. Additionally, the node's rate of energy consumption needs to be taken into account. The node that consumes more energy should typically be charged first.

The author's in [31] predicting a nearest-job-next with pre-emption method for determining the MC's charge decision. The charging priority of various nodes is adjusted by using two warning thresholds in the double warning threshold with double pre-emption algorithm [32] proposed in the same year. Additionally, [33] presented a primary scheduling algorithm that disregards the impact of choosing inefficient nodes and takes into account the closeness and urgency of balanced charging. For large-scale WRSNs, it was suggested a method of scheduling following secular dimensional charging that determined the node's death duration based on its power level and changed the charging sequence in accordance with the dead time [34]. This algorithm considered how charging performance might be affected by adjustments in the network architecture, node failures, and other un-predictabilities.

Additionally, the continuous accumulation of stochastic energy use is what leads to the node's charging request. The node's energy will run out quickly if its charging request is not fulfilled promptly. Real-time operations are necessary in WRSNs because unanticipated events can occur at any-time and anywhere, especially when the sensors are spread out across a large region [35]. Event-detection failure could result from any node running out of energy, so this should be prevented.

3. GROUNDWORK

3.1 *Outline of fuzzy logic*

Fuzzification, fuzzy logic controller, and defuzzification are the three functional components of a fuzzy logic system. During fuzzification, membership functions that are often utilised are used to convert inputs from their crisp form to their fuzzy form. The abbreviation and description are given in table 1 which are used in this work.

Table 1. Imported Notation

Abbreviation	**Description**
S_{ni}	Node of sensor
$M(i)$	M represents number of nodes
$N_{coverage}(i)$	Traversing nodes of mobile charging
E_{max}	Maximum capacity of nodes
E_{mc}	Capacity of the mobile charging battery
$D(Si, mc)$	Distance between two nodes
$D_{max}(BS)$	Distance from base station to node
CN_{si}	Node density
RE_{si}	Residual energy

!	Charging threshold of the MCs
SP_{si}	Scheduling probability of si
$N_{coverage}(i)$	nodes during a charging tour
$RE(mc)$	Mobile charger remaining power
ECR_{si}	Rate of power absorption
E_{move}	Travelling power absorption
$C_{thres}(si)$	Charging threshold
pr_{si}	Demand power acquired per sec by si from mobile charger
ECR_{max}	Maximum energy consumption rate of any node
RE_{max}	Peak energy of a node
CN_{max}	Maximum critical node density of any node
D_{max}	Higher distance in network among any two nodes.
$T_{coverage}(i)$	Time to recharge
Q_{req}	Demanding requests are gathered in form of queue

A rule base made up of the linguistic phrases "IF {set of inputs} - THEN {outputs}" is used by the fuzzy logic controller to make choices. The formulation for a fuzzy rule S_i with m inputs and 1 output is as follows:

$$S_i = IF(J_1 \; is \; B_{i1} \; AND \; J_2 \; is \; B_{i2} \; \ldots\ldots\ldots\ldots\ldots AND \; J_m \; is \; B_{im}) \; THEN \; (O \; is \; C_i) \quad \text{(eq. 1)}$$

Where $\{J_1 J_2, \ldots . J_m\}$ denote the input linguistic variables and O is the output linguistic variable. Here,$\{B_{i1,} B_{i2} \ldots\ldots\ldots\ldots . . B_{im}\}$ and $\{C_i\}$ are used to indicate the linguistic values for the input and output variables, respectively.

The following evaluation is made of the fuzzy outputs evaluated as membership function (δ) using the fuzzy S_i rule (using and Eq. (1)):

$$eval(S_i): (\delta_{Ai1}(J_1) \; AND \; \delta_{Ai2}(J_2) \; AND \; \ldots\ldots AND \delta_{Ai1}(J_{Aim})) \rightarrow \delta_{Bi}(O)_2) \quad \text{(eq.2)}$$

Notably, fuzzy logic controllers substitute conventional T- operators like MAX, MIN, and complement for combination operators as OR, AND, and NOT:

$$\{\delta_{Ai1}(J_1) \; AND \; \delta_{Ai2}(J_2) = \delta_{Ai \cap Aj}(J_{ij}) = MIN((\delta_{Ai}(J_i), \delta_{Aij}(J_j))\} \quad \text{(eq. 3)}$$

$$\{\delta_{Ai1}(J_1) \; OR \; \delta_{Ai2}(J_2) = \delta_{Ai \cup Aj}(J_{ij}) = MAX((\delta_{Ai}(J_i), \delta_{Aij}(J_j))\} \quad \text{(eq. 4)}$$

$$NOT\{\delta_{Ai}(J_i) = \delta_{Ai}\sim\} = 1 - \delta_{Ai}(J_i) \quad \text{(eq. 5)}$$

The commonly utilised crispification technique (i.e., centre of gravity) is then employed to transform the consolidated fuzzy result into its sharp version as follows:

$$Center\ of\ Gravety(CG) = \frac{\sum_{j=1}^{p} z_j \times \delta_C(z_j)}{\sum_{j=1}^{p} \delta_C(z_j)}$$

(eq. 6)

Where $\delta_C(Z_j)$ is the updated membership functions of the fuzzy output set C and p is the adjusted fuzzy output that spans the X-axis. is the updated membership functions of the fuzzy output set C and p is the adjusted fuzzy output that spans the X-axis. It should be noted that the suggested DCSR-FL method makes use of Eqs. (2)–(6).

3.2 *System description*

A WRSN is seen as being configured by the framework of numerous WCVs. The fig. 1 showed the on demand charging architecture. The construction of architecture has several sensors with identical battery capacities which have randomly dispersed in region with WCVs. Both WCVs and nodes come with limited-capacity batteries and GPS modules (or other localization tools). Nodes' main responsibility is to perceive, gather, and communicate ambient information. The default protocol, which uses directed diffusion, is used by the nodes to communicate. Furthermore, the measurement of energy level of sensors, threshold value is fixed. The running WCVs can go around the whole monitored zone and refuel for the nodes making the charging requests having below threshold energy.

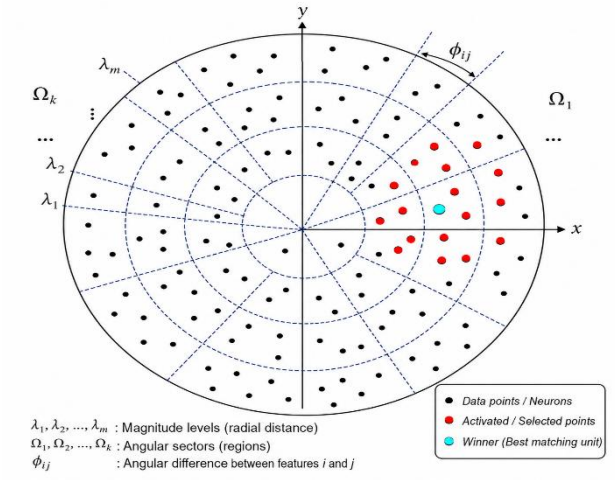

Figure 1. Architectural framework of numerous sensors

Imagine a WRSN with the following components: (i) randomly distributed 'N' number of sensor nodes; (ii) Homogeneous MCs which are k (> 1); (iii) Base Station (BS), which is in charge of maintenance and other MC-related functions in addition to collecting sensory data. The BS is in charge of assigning the MCs to tasks and has the ability to swiftly charge an MC's battery. Rechargeable battery with a En_{max} maximum energy capacity of node.

The work has assumed that the BS is aware of the locations of every node and that every node has the same chance of experiencing an event. Additionally, throughout each cycle of data gathering, the nodes continually detect their surroundings and relay the perceived information to the BS. It is also believed that there are no isolated nodes in the network [36]. Each MC has an energy capacity En_{mc} that may be utilised for both its movement purposes and another is energy transfer to neighbouring nodes. The system operates in the manner described below. Every node keeps track of how much energy is left in it. A node will submit a charging request to the approved MC if its energy level drops below its charging threshold, which varies according on the node's rate of energy consumption. The ID and location of the node are included in the charging request messages. The MC chooses the nodes' charging schedule based on network data. The sequence in which an MC visits asking nodes to recharge them is known as a charging schedule, or$D_{schedule}$. It may be demonstrated mathematically as follows.

$$D_{schedule} = \{BS \rightarrow S_j \rightarrow S_{J+1} \dots\dots\dots S_r\} \qquad \text{(eq .7)}$$

S_{j+1} Has recharge after S_j, where r is the total number of asking nodes in the request queue. This work employ the same energy model as [21], which allows nodes to use energy for processing, sending, and receiving operations. The nodes' energy consumption characteristics, however, are unknown beforehand. Depending on the underlying

application or routing protocol, sensor nodes may have varying energy consumption due to their disparate traffic loads. This demonstrates the fluctuating and dynamic energy consumption rates of the sensor nodes. It should be underlined that while employing the technique of energy notification messages described in [37], all MCs are needed to regularly be aware of this dynamic rate of energy consumption of the nodes. The charging energy that $S_{i,}$ (i.e., $P_r(S_i)$ got in accordance with the charging model in [21] is computed as:

$$P_r(S_i) = \{\delta \times D_{rate} \;\; ; \quad if\ E(S_{i,}mc) \leq D_r\ 0, \qquad ; \quad if\ E(S_{i,}mc)E\ x > D_r \qquad \text{(eq. 8)}$$

Where $E(S_{i,}mc)$ represents the distance between si and an MC and (0 1) is the competence measure of the charging energy. In this study, it is assumed that there is no variation in the recharging energy between the nodes because an MC typically only has a modest charging range (D_r =2.7 meter); hence, $t_{charge}(CN(S_{i,}))$ is calculated as follows:

$$t_{charge}\left(CN(S_{i,})\right) = max_{S_i \epsilon CN(S_i)}(t_{charge}(S_i)) \qquad \text{(eq.9)}$$

Where $t_{charge}(S_i)$ is time an MC needs to charge S_i node. In this study, there is no need to address the routing of billing requests. The $t_{charge}(S_i)$ is defined as

$$t_{charge}(S_i) = \frac{F_{max}}{P_r(S_i)} \qquad \text{(eq.10)}$$

For the sake of simplicity, it is assumed that the routing time of charging requests pales in contrast to the MC's travel and charging times [38].

4 PROPOSED METHODLOGY

The suggested concept's fundamental operational phases are as follows: Following network initialization, it (1) splits the network into equal halves such that the MCs are each subject to an equal charging load from the sensor nodes, using the nodes' heterogeneous energy consumption rate, (2) generates a dynamic charging threshold for them, and (3) establishes the nodes' charging threshold. the application of fuzzy logic to jointly assess multiple network properties in order to choose the appropriate node to be charged next. The flow chart depicting all of the aforementioned actions is depicted in Figure 2.

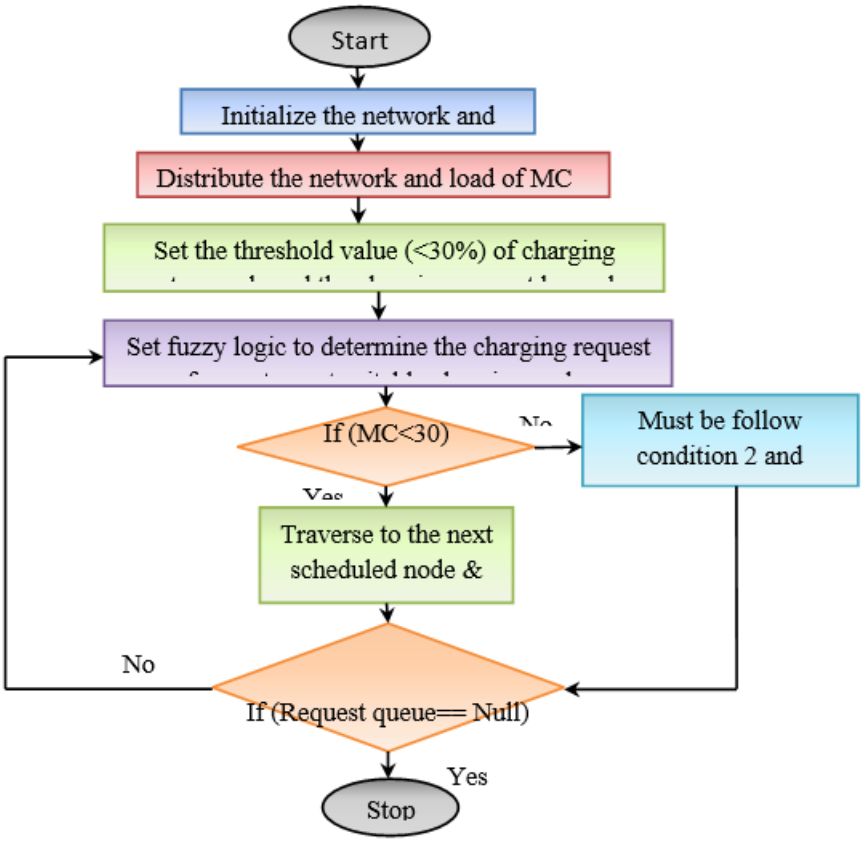

Figure 2. Data flow diagram of proposed work.

4.1 *Distribution of Network for MC*

The purpose of dividing the network is to divide the MCs into k distinct areas, each of which will contain only one MC. The major goal is to equally distribute the network's nodes' traffic loads in order to balance the charging loads placed on each MC. This gives nodes with irregular energy consumption rates a timely charging response. It should be noted that the suggested method is unaffected by the network's size or density. Additionally, the BS executes periodic network segmentation using the suggested methodology in order to properly manage changing network dynamics. Any common routing approach may be used to predict the traffic loads on all nodes. The data packets send to the node's traffic load is done using the BS during the course of a data collection cycle. It is presumed that the BS is situated in the network's core. Let TTL stand for the network's overall traffic load and RTL for a specific region's traffic load. Generally speaking, the following two requirements must be met for effective network partitioning:

(1) $IF\ MOD(TTLN; m) == 0$: When the area Traffic Load of Network ("RTLN") of each area is equal to or greater than the Total Traffic Load of Network ("TTLN") efficient traffic load balancing threshold, the network dividing $\frac{TTL}{m}$, the network partitioning will efficiently load balance traffic.

(2) $IF\ MOD\ (TTLN;\ m)\ \neq 0$, Effective traffic load balancing will be achieved by network partitioning when each of the mod $(TTLN;\ m)$ regions has $RTLN = (TTLN/k) + 1$ and the remaining regions have $RTLN = TTLN/m$.

This is how our network splitting strategy operates. A base axis line from the BS is taken into consideration for the first partitioned region and meets the rectangle network horizontally shown in Fig. 3(b). The base axis line's distance from each node is then calculated. The calculations in Fig. 3(c) are used to determine the angle between the nodes. Following that, they are all sorted in a non-decreasing order. In non-decreasing order of their angular distances up to $RTLN \leq \lfloor \frac{TTLN}{m} \rfloor$, the nodes are now picked one by one. The first area is home to all nodes that meet this requirement. Similar to that, this procedure is continued until k number of regions is generated and all nodes are

covered. The TTLN of the network is 40. Assuming n = 5, the RTLN ought to be equal to $\lfloor \frac{40}{5} \rfloor = 8$. Until a node's RTLN equals 8, it has been selected, in non-decreasing order of angular distance. Due to their RTLN of 8, the nodes 5, 8, 15, 19, and 22 are chosen to be a part of the first region. All five regions may be built by repeating this method in a similar fashion. The different network partitioning approaches are given in figure 3.

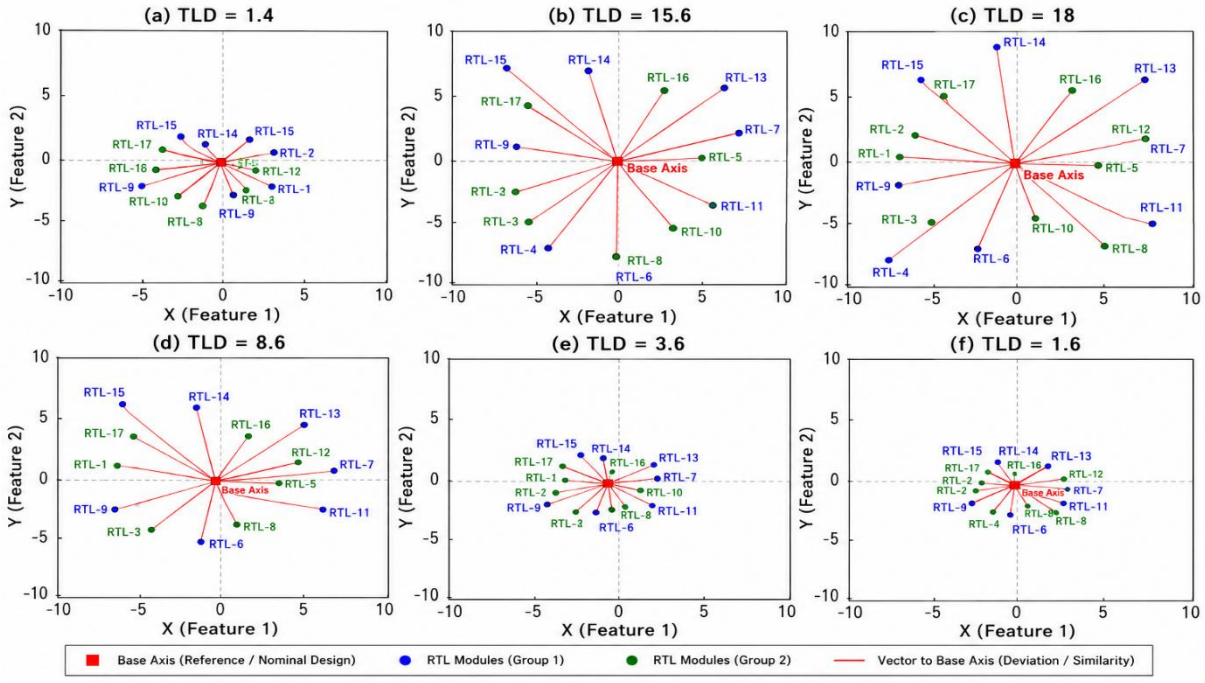

Figure. 3 In k = 5, (a) 0° axis, (b) 60° axis, (c) 120° axis, (d) 180°axis , (e) 240° axis, and (f) 300°axis.

The final partitions, with RTLN = 8; 6; 6; 7; and 13, are displayed in Fig. 3(b). The aforementioned example illustrates how a sparse "WRSN" may come upon an instance where RTL is not evenly spread over the regions. Using multiple base axis lines may also lead to improved traffic load distribution as network density rises. Given the aforementioned information, our method divides the network by multiple base axis lines at different angular rotations. Another dense network situation is one in which the base axis is rotated by 60 degrees to generate $\frac{360}{60} = 6$ degrees. Figures 4(a) through 4(f) depict the six distinct partitioning instances that result from 60°. The total deviation of the load is represented as

$$TLD = \sum_{j=0}^{m} \quad T\left|RTL_{avg} - RTL_j\right| \qquad \text{(eq. 11)}$$

Where RTL_j and RTL_{avg} stand for the ith region's RTL and the overall average RTL, respectively. As shown in figures 4(a)–4(f), this study selects the partitioning instance with the lowest TLD, which is also the most effective partitioning. Furthermore, in an exceptionally dense WRSN, a little modification to the base axis may result in a different partitioning conclusion. In order to get the best partitioning results with almost equal RTL distribution, our technique suggests changing the base axis by 1° for each division. In rare situations, the instance with the lowest TDD may be chosen while several instances having the minimum TLD values. The network's total density deviation, or TDD in this context, is defined as

$$TDD = \sum_{j=1}^{l} \quad R\left|RDN_{avg} - RDN_j\right| \qquad \text{(eq. 12)}$$

Where RDN_j stands for “Regional Node Density” and RDN_{avg} stands for “Average Regional Node Density”. Any instance with a minimal TDD can be chosen if there is minimum TDD. The TLD of every (360°)/(1°) instance for a random network condition is indicated in Fig. 5(a). The figure shows the base axis angles for the instances constructed with a minimum TLD of 1.6 is shown in the image by the red-highlighted boxes. Here, just two

rudimentary TLD examples are shown (Figs. 4(b) and 4(c)). Fig. 4(c), which has a minimum TDD of 4, is used to determine the final division. Fig. 4(c) displays the traffic load distribution among the five divided parts. Additionally, this instance has the best node density distribution across all of its partitions in comparison to other instances. Following network partitioning, One MC is distributed by the BS to each region, and the nodes are informed of its ID so they may send charging requests to it. Additionally, every MC is aware of where the nodes are in its particular zone

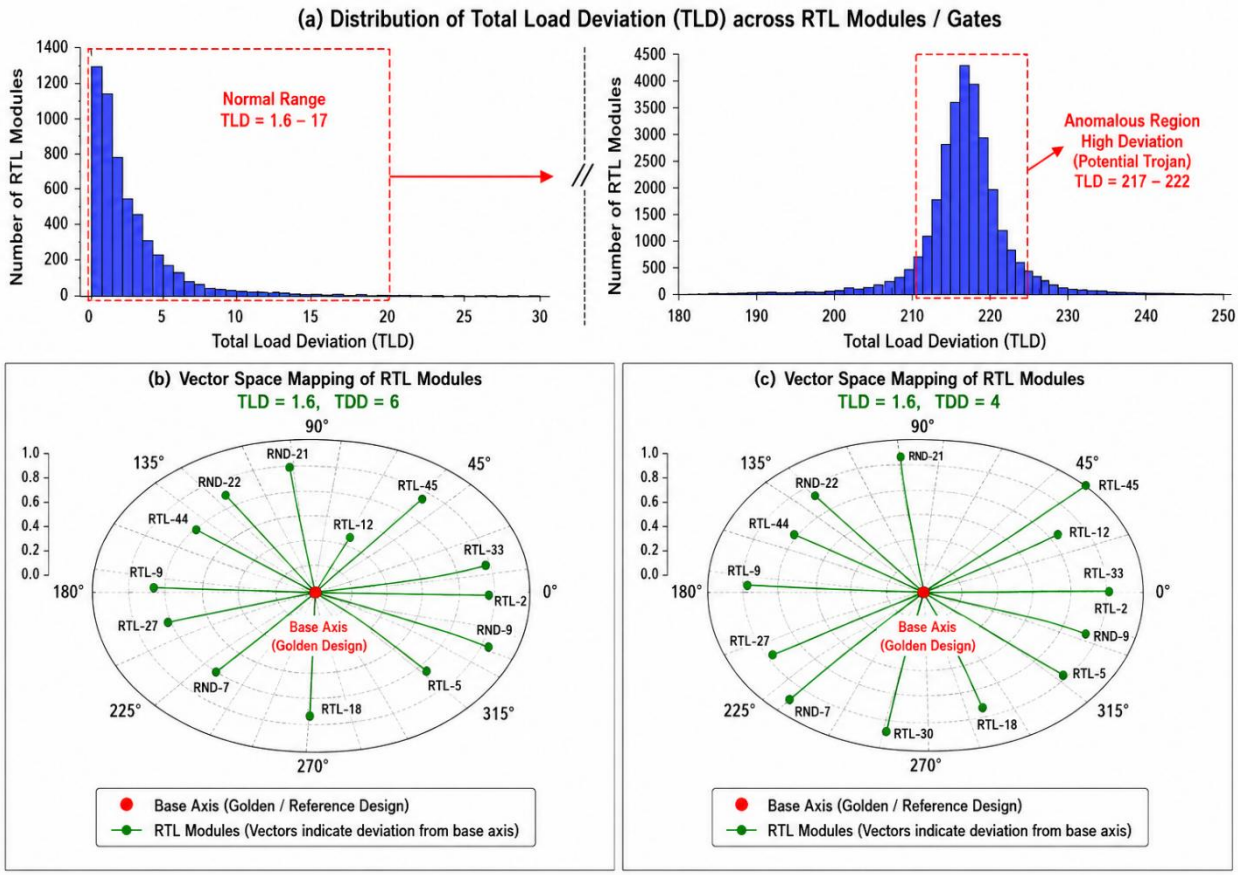

Figure 4: A network partitioning strategy with k = 5 shows the following partitioning instances: two partitioning instances: (a) one with TLD = 1:6 and TDD = 4, and (b) one with TLD = 1:6 and TDD = 4.

4.2 Origination of Threshold value for Sensors

In the network, unpredictable occurrences invariably happen seldom, and as a result, node energy consumption rates vary substantially. Fixed charge thresholds for nodes are inappropriate in this situation for dynamic networks. An extremely low threshold causes charging request responses to take longer, which causes more nodes to experience early death. On the other side, a threshold that is set too high reduces the efficiency of charging since it takes too long to move because charging requests come in more frequently. To improve charging efficiency in the network, it is thus worthwhile to investigate defining an appropriate charging threshold for the nodes. The following adaptive method for determining the charge threshold is suggested as a result of the facts mentioned above.

Let's have a look at the j^{th} region; where $N(j)$ denotes region's number of nodes and $M_{coverage}$ shows the count of nodes an MC may pass over during a recharging trip. Let Ecoverage represent the overall energy expended by the MC to go to $M_{coverage}(j)$ nodes,

Where $M_{coverage}$ is defined as

$$F_{coverage} = (M_{coverage}(j) + 1) \times E_{average} \times F_{move} \quad \text{(eq. 13)}$$

Where

$$E_{average} = \frac{1}{M_j \times (M_j+1)} \sum_{y=1}^{M_j+1} \quad \sum_{z=1, y \neq z}^{M_j+1} \quad E(t_y, t_z) \qquad \text{(eq. 14)}$$

Here, $E(t_y, t_z)$ signifies the "Euclidean Distance" between two nodes, and E_{move} represents the energy motion. $E_{average}$ between any two nodes, is the typical Euclidean distance. $M_{coverage}(j) + 1$ Represents $F_{coverage}$ nodes including the BS.

4.3 *Charging schedule determination*

Each MC determines the billing schedule for its regional nodes, as was already mentioned. S_{req} stores the charging requests that an MC receives from its regional nodes. The MC logs the values for each network characteristic using the network data. It should be noted that the total number of requesting nodes that are within a node's charging range may be used to calculate the critical node density for that node. The scheduling likelihood of each inquiring node is then calculated using the FIS to choose the optimal node to charge next. The MC moves to that node and supplies it with power. When charging is complete, the MC removes the recharged nodes from theS_{req}. Likewise, each asking node is scheduled and compensated separately. The charging schedule is stated to be determined iteratively in a real-time, dynamic process. It waits until the prior charging schedule is complete if new charging requests are made in the interim. The following two scenarios are taken into account by an MC before serving a scheduled node S_i.

Scenario 1. Let, $E_{max}(BS)$ represents the maximum distance of a node from the BS. If the remaining energy of the MC exceeds the threshold value μ where($\mu \geq E_{move} \times E_{max}(BS)$), then it keeps on recharging the planned nodes.

Scenario 2. If the MC is less than, the nodes in Q_{req} are checked to see if they comply with the next restriction.

$$E_{move} \times E\left(e_{s_i}, BS\right) \leq RE(MC)(t) - \left(E_{move} \times E\left(e_{s_i}, MC\right)\right) - (E_{max} - ER(s_i)(t + t')) \qquad \text{(eq.15)}$$

$RE(MC)(t)$ is the amount of energy the MC has left at that moment. $ER(s_i)(t + t')$ is the energy that s_i has left at time $t + t'$, where t, t' is the moment that MC arrives at the node s_i. In conclusion, after recharging the next scheduled node, the MC first assesses if it has sufficient energy to go to the BS. By using the suggested method, the candidate nodes from which the recharge of the ensuing node is planned are those nodes that satisfy the constraint. If no asking node complies with the aforementioned restriction, The MC declines any further requests for charging and instantly goes back to the BS for recharging.

Next, describe how to use the DCSR-FL method to identify which node will be charged next. Accordingly, the FIS's four inputs and one output in our design are remaining "Energy (RE)", "Distance to node (D)", "Critical node density (CN)", "Energy Consumption Rate (ECR)", and "Scheduling Probability (SP)". The FIS design is shown in Fig. 5, and Procedure FUZZY describes the pseudo-code it employs. The membership functions for trapezoidal and hexagonal triangles are shown in Figs. 6 and 7, respectively, along with examples of how these fuzzy variables may be represented by a variety of fuzzy linguistic values. In Tables 2 and 3, respectively, the linguistic values for the input and output fuzzy variables are displayed.

Table 2. Linguistic values for the input variables and the accompanying membership function range

Variables	The function range of Linguistic values	
Residual Energy (RE)	"Low" (L)	[0,0,0.3*RE_{max}, 0.6*RE_{max}]
	"Medium" (M)	[0.3*RE_{max}, 0.6*RE_{max}, 0.9*RE_{max}]
	"High" (H)	[0.6*RE_{max}, 0.9*RE_{max}, RE_{max}, RE_{max}]
Distance to MC (D)	Minimum (Min)	[0,0,0.25*Di_{max}, 0.35*Di_{max}]
	Average (A)	[0.25*Di_{max}, 0.35*Di_{max}, 0.65*Di_{max},
	Maximum (Max)	0.75*Di_{max}]
		[0.65*Di_{max}, 0.75*Di_{max}, Di_{max}, Di_{max}]
Critical Node Density (CND)	Minimum (Min)	[0,0,0.25*CND_{max}, 0.35*CND_{max}]
	Average (A)	

	Maximum (Max)	$[0.25*CND_{max}, 0.35*CND_{max}, 0.65*CND_{max}, 0.75*CND_{max}]$
		$[0.65*CND_{max}, 0.75*CND_{max}, CND_{max}, CND_{max}]$
Energy Consumption Rate (ECR0	L	$[0,0,0.3*ECR_{max}, 0.6*ECR_{max}]$
	M	$[0.3*ECR_{max}, 0.6*ECR_{max}, 0.9*ECR_{max}]$
	H	$[0.6*ECR_{max}, 0.9*ECR_{max}, ECR_{max}, ECR_{max}]$

Table 3: Output variable with its membership function ranges and linguistic values

Variable	Function range of Linguistic values	
"Scheduling Probability of Node" (SPN)	"Very Low" (VL)	[0, 0, 0.1, 0.16]
	L	[0.1, 0.16, 0.32, 0.6]
	M	[0.40, 0.4, 0.6, 0.65]
	H	[0.5, 0.65, 0.85, 0.9]
	"Very High" (VH)	[0.8, 0.9, 1]

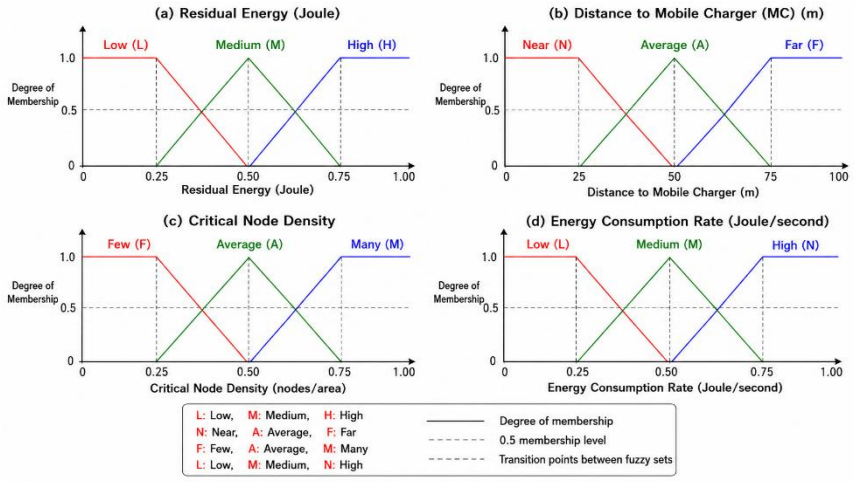

Figure 5 Membership functions for fuzzy inputs the amount of residual energy, the distance to the MC, the density of the critical nodes, and the rate of energy consumption.

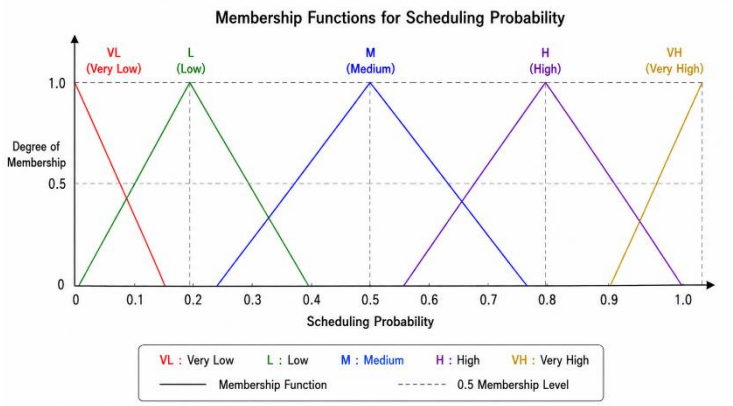

Figure 6. Scheduling probability of Fuzzy output membership function.

According to Table 4, the proposed scheme's whole rule set is made up of rules. This study has transformed the crisp data inputs to the fuzzy inputs using the trapezoidal and triangular membership functions offered in Eqs. (18)

and (19). Using Eqs. (18) and (19), The aforementioned crisp inputs are used to compute the fuzzy inputs of various linguistic variables.

Table 4. Calculate fuzzy input from crisp input by using the input membership function.

Given crisp input, calculate the fuzzy input			
L = 1	"Minimum" (Di) = 0.942	"Minimum" (CND) = 1	L (ECR) = 1
M = 0	"Average" (Di) = 0.058	"Average" (CND) = 0	M (ECR) = 0
H = 0	"Maximum" (Di) = 0	"Maximum" (CND) = 0	H(ECR) = 0

The updated fuzzy outputs from Table 4 are used to create the aggregated fuzzy output. The fuzzy membership ranges of SP that extend across intervals include $VL = NULL$, $L = [0.1, 0.1029, 0.3971, 0.4]$, $M = [0.35, 0.3971, 0.6029, 0.65]$, $H = NULL$, and $VH = NULL$, to name just a few. Lastly, the output called crisp (i.e., defuzzification point) from the combined fuzzy output is calculated as 0.509 using the defuzzification technique (Eq. (6)). The crisp output is the total of each node's SP value, sometimes referred to as scheduling probability. The node with the same SP value that is closest to the recharge point if numerous nodes are assigned greater priority. The pseudo-code for Algorithm 1 shows the proposed course of action.

Algorithm 1. Determination of Charging Schedule Request using Fuzzy Logic (DCSR-FL)

Input: Take input as Q_{req} , RE_{Max} , D_{max} , CRN_{max} , and $ECNR_{max}$,
Output: Charging schedule $as\ ch_{schedule}$

1. Send signal $S_i(p)$ to MC as cluster head
2. Set $Q_{req}(i) \longrightarrow RES_{max} + DI(S_{i,}MC) \quad + CRN_{S_i} + ECNR_{max}$
3. Check if $(Q_{req}(i)\ != NULL)$
   Do
   FUZZY $(RES_{max} + DI(S_{i,}MC) \quad + CRN_{S_i} + ECNR_{max})$
   Set a higher value of $S_i\ for$ selective MC where $i = 1,2,3, \ldots \ldots . . n$ and set the path from MC to MC
4. Print□□schedule probability of S_i
5. Set the schedule $ch_{schedule} = MC_{schedule} \cup S_i$
6. Print□schedule $ch_{schedule}$ and remove $Q_{req}\ and$ update the queue

Return □ $ch_{schedule}$

5. SIMUATION ANALYSIS

Numerous simulations have been achieved to confirm the gains of the recommended strategy. The proposed DCSR-FL system has been compared to and evaluated using the charge schemes reported in [21] and [20]. The systems [21] and [20] both conform to the on-demand multi-node charging design and utilise a number of MCs. Let's use the schemes [20] as UCMC and [21] as OMC TSP to show the results. For good results it is believed that there isn't any combined "Electro Magnetic Radiation (EMR)" among nearby MCs. This work generally takes into account three performance measures when evaluating the recommended scheme's efficacy: survival rate, average charging delay, and energy consumption efficiency.

5.1 Simulation environment

This work has taken into account a WRSN with number of nodes from 400 to 1000 that all distributed at random across a 100 by 100 m2 area. At the heart of the network is where the BS for the simulation, we've used the following parametric assumptions. Each node has a 10:8 KJ power capacity [27]. Each MC has a maximum energy of 4000 KJ [27]. The charging rate for each MC is 5 J/s [21] and 0:68 [17]. Each MC moves at a speed of vmc and uses 600 J of energy per meter [24], [27]. MATLAB version R2016a is used to execute the simulations, along with an Intel Core 2 Duo processor and 4GB of RAM. For fair comparisons, the findings were shown in each figure as the average of 20 random simulated cases. Table 5 displays the significant simulation parameters and their values.

Table 5. Parameters of Simulation

Parameter	**Value**

"Network Region" (NR)	$100 \times 100\ m^2$
"Number of Nodes" (N)	$300 - 1000$
"Number of MCs" (k)	6
"Battery capacity of nodes" (E_{max})	$10.9\ KJ$
"Battery capacity of MCs" (E_{mc})	$5000\ KJ$
Moving energy consumption rate (E_{move})	$700\ J/m$
Moving speed of MC (v_{mc})	$1 - 6\ m/s$
Charging range (C_r)	$1.7\ m$
The charging rate of MCs (C_{rate})	$6\ J/s$
"Charging energy efficiency rate" (n)	0.70
"Simulation time"	$150\ hours$

5.2 Evaluation of Proposed Model

This section shows different network configurations result, such as the number of nodes, the length of the simulation, and the MC's movement speed, affect performance measures.

5.2.1 Energy usage efficiency

The "Energy Utilisation Efficiency (EUE)" is the ratio of the total energy transmitted from the BS to the MCs to the total energy obtained by nodes [39]. The EUE is crucial for achieving promising charging performance. More nodes are getting punctually charged when the EUE is higher. As can be shown from Figure 8 and figure 9, as the MC's movement speed, simulation duration, and node count increase, correspondingly, the EUE of DCSR–FL is comparatively high when compared to those of the other two schemes. This demonstrates how the recommended method performs better than others. This is explained by the fact that the DCSR-FL fuzzy logic tends to make efficient scheduling judgments that provide more nodes the opportunity to charge simultaneously. It maximises the quantity of energy sent to the nodes as a consequence. However, unlike DCSR-FL the charging load of MCs for UCMC and OMC TSP is inefficiently balanced. Additionally, these schemes lack effective selection criteria for selecting the correct node for charging. As a result, the EUE is decreased since fewer nodes are punctually recharged. Given that the MCs with more nodes receive more charging requests this makes it reasonable.

5.2.2 Survival rate

The percentage of nodes that the MCs successfully charged to all nodes that were seeking is known as the survival rate (SR). Figures 8 and 9 show the comparative results for SR with various simulation times and MC movement rates, respectively. Increasing charging efficiency requires a network with a high SR since it assures connectivity and stability. To handle additional requests, the DCSR-FL provides scheduling of the nodes by combining various criteria [40]. Additionally, each MC completes the recharging chores faster thanks to the load-balanced network partitioning. As a result, more nodes are charged, which raises the SR. In addition, as the simulation in figure 9 proceeds, the SR decreases. Additionally, as shown in figure 9, the rate of survival between different schemes dramatically decline in comparison to those of the proposed DCSR-FL scheme. This is so because the compared schemes don't take into account fixed charge thresholds for the nodes or make scheduling decisions by combining different network properties. This ignores the necessity of recharging, resulting in the more crucial nodes frequently dying in the case of a high volume of charging requests. Similar to this, as the movement speed of the MC increases the SR of all the simulated schemes increases. The argument is that by moving more swiftly, the MC can service more asking nodes. Since more nodes have been successfully charged overall as a result, each of these schemes now have a higher survival rate.

5.2.3 Suspension of Average charging

"Average Charging Latency (ACL)" is the time interval between the charging requests to its completion time by the MC. The ACL is lower, which reduces the amount of time other crucial nodes must wait before dying from energy exhaustion. As seen in Figure 8, the ACL of the DCSR-FL scheme is consistently lower than that of others with different numbers of nodes and simulation periods. Additionally, the network is distributed evenly by balancing the traffic load on the requesting nodes, which reduces the load on the MCs and speeds up the response time for charging the nodes. As a result, the MC typically serves a greater volume of requests while lowering the network's ACL. Additionally, adaptive charging thresholds assist nodes in timely charging request transmission while minimally delaying response time. Also, modern scheduling methods fail to take the aforementioned considerations into account and produce poor scheduling results. Additionally, the network's imbalanced charging workload for each MC causes the ACL to rise sharply [35]. The ACL achieved by the simulated systems for various MC movement speeds is plotted in Figure 7. The ACL reduces as MC speed rises, as is obvious; however, the rates at which it decreases vary. This is because the ACL gets smaller as MC's speed increases. After all, it needs to travel less distance to satisfy the requesting nodes. As the MC moves at f1, f2, and f3 gm=s, the ACL of each scheme initially decreases at the same rate. The DCSR-FL scheme's ACL drops more quickly as MC speed rises. Among those reported, the ACL for DCSR-FL is likewise the lowest, being 6% lower than for UCMC and 9% lower than for OMC_TSP.

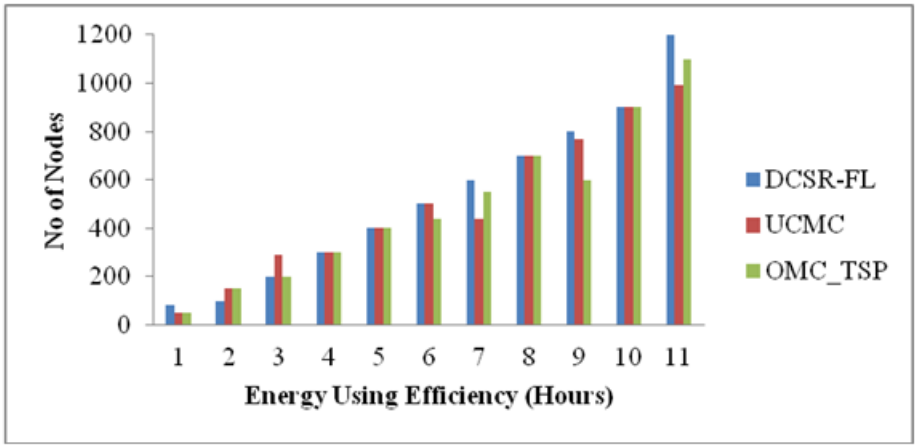

Figure 7. Performance comparison of energy uses efficiency

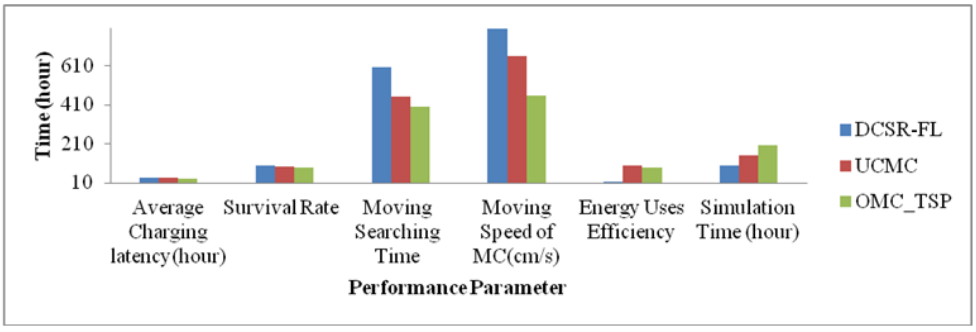

Figure 8 Performance comparisons of average charging latency, Survival rate, Moving searching time, Moving speed of MC, Energy uses efficiency and simulation time.

5.2.4 Statistical Validation of Data Analysis

In this part, hypothesis testing is done to examine whether the simulation findings have statistical significance. The same function is carried out using analysis of variance (ANOVA) [34], [36]. ANOVA, a statistical technique, is frequently used to distinguish between two or more means. It aids in figuring out if the null hypothesis, "H_y0: The given groups have the same means," may be thoroughly rejected. Let the G-statistic indicate the outcome of the ANOVA test. The G-statistic must be bigger than the F1 score value and the p-value must be below the significance level in order to reject the null hypothesis. There are 20 samples of each scheme within the same network instance were subjected to the ANOVA test with = 0:05 on each performance metric. The null hypothesis in this study is "$H_{y0}: \rho_{FLCSD} = \delta_{TDMC} = \delta_{PD\_MC}$" A different variation is "$H_{y1}: \rho_{FLCSD} \neq \delta_{TDMC} \neq \delta_{PD\_MC}$")". The ANOVA test

results, together with the F-statistic, P-value, and F-critical values, are displayed in Table 6 for your convenience. Both of the aforementioned requirements are met, according to the findings analysis of this investigation (the p-value is significantly below 0:05 and the F-statistic is bigger than the F-critical).

Table 6. Result of the ANNOVA test

Performance Metric	F-Statically	P-Value	F-critical
Energy use efficiency	11.5134543	2.11593E-05	3.15874271
Survival Rate	16.5856473	3.56752E-20	3.17824596
Average charging latency	12.39063451	2.70701E-05	3.15884271

This study has thus found that the null hypothesis is incorrect. This confirms how important a part each exhibited religious auxiliary played in the system that was decided by all the simulate. Additionally, 97% confidence suggestions for each performance proposal's enrolment, as assessed by the simulation, were offered.

6. CONCLUSIONS

The demand-side In order to concentrate on the MC's limited power supply and multi-node energy transmission capacity, WRGN faces scheduling issues with numerous MCs. This research primarily established MC in order to show a potential network division method in a drive-balanced way. The adaptive recharging levels for the nodes are now calculated mathematically, preventing the MCs from charging the nodes unjustly. Finally, the Mamdani Fuzzy Inference System was employed to forecast the nodes' charging schedules. This system intelligently takes into account a number of factors, including energy consumption rate, important node density, distance to the MC, and residual energy. Numerous simulations have been performed to show how the suggested DCSR-FL strategy outperforms the most cutting-edge methods.

The results show that the FL-DCSR performs better than cutting-edge methods in terms of stability by increasing the number of nodes that survive and charging performance by achieving a short average charging delay and outstanding energy consumption efficiency. The statistical ANOVA test is used to further validate the simulation results. However, the coordination between the MCs for recharging the nodes and the MCs is not taken into consideration in the suggested method, which might further improve the charging performance, particularly in large-scale WRSNs. Plan to also look at novel multi-attribute decision-making approaches to include this functionality in our next work.

REFERENCES

1. M. Ayaz, M. Ammad-uddin, I. Baig, et al., “Wireless sensors civil applications, prototypes, and future integration possibilities: A review,” IEEE Sensors Journal, vol. 18, no. 1, pp. 4–30, 2017.
2. P. Kar and S. Misra, “Reliable and efficient data acquisition in wireless sensor networks in the presence of trans faculty nodes,” IEEE Transactions on Network and Service Management, vol. 13, no. 1, pp. 99–112, 2016.
3. S. Gao, H. Zhang, and S. K. Das, “Efficient data collection in wireless sensor networks with path-constrained mobile sinks,” IEEE Transactions on Mobile Computing, vol. 10, no. 4, pp. 592–608, 2010.
4. B. Fateh and M. Govindarasu, “Joint scheduling of tasks and messages for energy minimization in interference-aware real-time sensor networks,” IEEE transactions on mobile computing, vol. 14, no. 1, pp. 86–98, 2013.
5. S. Guo, Y. Shi, Y. Yang, and B. Xiao, “Energy efficiency maximization in mobile wireless energy harvesting sensor networks,” IEEE Transactions on Mobile Computing, vol. 17, no. 7, pp. 1524–1537, 2017.
6. A. Mehrabi and K. Kim, “General framework for network throughput maximization in sink-based energy harvesting wireless sensor networks,” IEEE Transactions on Mobile Computing, vol. 16, no. 7, pp. 1881–1896, 2017.
7. A. Kurs, A. Karalis, R. Moffatt, J. D. Joannopoulos, P. Fisher, and M. Solja˘ci´c, “Wireless power transfer via strongly coupled magnetic resonances,” science, vol. 317, no. 5834, pp. 83–86, 2007.
8. K. Kang, Y. S. Meng, J. Br´eger, C. P. Grey, and G. Ceder, “Electrodes with high power and high capacity for rechargeable lithium batteries,” Science, vol. 311, no. 5763, pp. 977–980, 2006.
9. M. Hu, Z. Chen, K. Peng, X. Ma, P. Zhou, and J. Liu, “Periodic charging for wireless sensor networks with multiple portable chargers,” IEEE Access, vol. 7, pp. 2612–2623, 2018.
10. L. Xie, Y. Shi, Y. T. Hou, W. Lou, H. D. Sherali, and S. F. Midkiff, “Multi-node wireless energy charging in sensor networks,” IEEE/ACM Transactions on Networking (ToN), vol. 23, no. 2, pp. 437– 450, 2015.
11. A. Kaswan, A. Tomar, and P. K. Jana, “An efficient scheduling scheme for mobile charger in on-demand wireless rechargeable sensor networks,” Journal of Network and Computer Applications, vol. 114, pp. 123–134, 2018.
12. L. He, L. Kong, Y. Gu, J. Pan, and T. Zhu, “Evaluating the on-demand mobile charging in wireless sensor networks,” IEEE Transactions on Mobile Computing, vol. 14, no. 9, pp. 1861–1875, 2015.

13. C. Lin, J. Zhou, C. Guo, H. Song, G. Wu, and M. S. Obaidat, “Tsca: A temporal-spatial real-time charging scheduling algorithm for on-demand architecture in wireless rechargeable sensor networks,” IEEE Transactions on Mobile Computing, vol. 17, no. 1, pp. 211–224, 2018.
14. C. Lin, Z. Wang, D. Han, Y. Wu, C. W. Yu, and G. Wu, “Tadp: Enabling temporal and distantial priority scheduling for on-demand charging architecture in wireless rechargeable sensor networks,” Journal of Systems Architecture, vol. 70, pp. 26–38, 2016.
15. Y. Shu, H. Yousefi, P. Cheng, J. Chen, Y. J. Gu, T. He, and K. G. Shin, “Near-optimal velocity control for mobile charging in wireless rechargeable sensor networks,” IEEE Transactions on Mobile Computing, vol. 15, no. 7, pp. 1699–1713, 2015.
16. L. Fu, P. Cheng, Y. Gu, J. Chen, and T. He, “Optimal charging in wireless rechargeable sensor networks,” IEEE Transactions on Vehicular Technology, vol. 65, no. 1, pp. 278–291, 2016.
17. A. Kurs, R. Moffatt, and M. Solja˘ci´c, “Simultaneous mid-range power transfer to multiple devices,” Applied Physics Letters, vol. 96, no. 4, p. 044102, 2010.
18. Authorized licensed use limited to: University of Melbourne. Downloaded on May 03,2020 at 14:58:49 UTC from IEEE Xplore. Restrictions apply. 1536-1233 (c) 2020 IEEE. Personal use is permitted, but republication/redistribution requires IEEE permission. See http://www.ieee.org/publications_standards/publications/rights/index.html for more information.
19. This article has been accepted for publication in a future issue of this journal, but has not been fully edited. Content may change prior to final publication. Citation information: DOI 10.1109/TMC.2020.2990419, IEEE Transactions on Mobile Computing 13
20. W. Xu, W. Liang, H. Kan, Y. Xu, and X. Zhang, “Minimizing the longest charge delay of multiple mobile chargers for wireless rechargeable sensor networks by charging multiple sensors simultaneously,” in 2019 IEEE 39th International Conference on Distributed Computing Systems (ICDCS). IEEE, 2019, pp. 881–890.
21. W. Xu, W. Liang, X. Jia, H. Kan, Y. Xu, and X. Zhang, “Minimizing the maximum charging delay of multiple mobile chargers under the multi-node energy charging scheme,” IEEE Transactions on Mobile Computing, 2020.
22. G. Han, H. Guan, J. Wu, S. Chan, L. Shu, and W. Zhang, “An uneven cluster-based mobile charging algorithm for wireless rechargeable sensor networks,” IEEE Systems Journal, 2018.
23. T. Rault, “Avoiding radiation of on-demand multi-node energy charging with multiple mobile chargers,” Computer Communications, vol. 134, pp. 42–51, 2019.
24. R. V. Kulkarni, A. Forster, and G. K. Venayagamoorthy, “Computational intelligence in wireless sensor networks: A survey,” IEEE communications surveys & tutorials, vol. 13, no. 1, pp. 68–96, 2011.
25. L. Jiang, X. Wu, G. Chen, and Y. Li, “Effective on-demand mobile charger scheduling for maximizing coverage in wireless rechargeable sensor networks,” Mobile Networks and Applications, vol. 19, no. 4, pp. 543–551, 2014.
26. W. Liang, W. Xu, X. Ren, X. Jia, and X. Lin, “Maintaining large-scale rechargeable sensor networks perpetually via multiple mobile charging vehicles,” ACM Transactions on Sensor Networks (TOSN), vol. 12, no. 2, p. 14, 2016.
27. C. Lin, D. Han, J. Deng, and G. Wu, “P 2 S: A primary and passerby scheduling algorithm for on-demand charging architecture in wireless rechargeable sensor networks,” IEEE Transactions on Vehicular Technology, vol. 66, no. 9, pp. 8047–8058, 2017.
28. W. Xu, W. Liang, X. Lin, and G. Mao, “Efficient scheduling of multiple mobile chargers for wireless sensor networks,” IEEE Transactions on Vehicular Technology, vol. 65, no. 9, pp. 7670–7683, 2016.
29. Y. Ma, W. Liang, and W. Xu, “Charging utility maximization in wireless rechargeable sensor networks by charging multiple sensors simultaneously,” IEEE/ACM Transactions on Networking, no. 99, pp. 1–14, 2018.
30. N. Gharaei, Y. D. Al-Otaibi, S. A. Butt, S. J. Malebary, S. Rahim, and G. Sahar, “Energy-efficient tour optimization of wireless mobile chargers for rechargeable sensor networks,” IEEE Systems Journal, 2020.
31. S. Upadhyay, M. Kumar, A. Kumari, R. Kranti, “Feature Extraction Approach for Speaker Verification to Support Healthcare System using Blockchain for Data Privacy”, Computational and Mathematical Methods in Medicine, Vol. 2022, pp. 1-12, July 2022.
32. L. Mo, A. Kritikakou, and S. He, “Energy-aware multiple mobilz chargers coordination for wireless rechargeable sensor networks,” IEEE Internet of Things Journal, vol. 6, no. 5, pp. 8202–8214, 2019.
33. S. Upadhyay, M. Kumar, A. Upadhyay, S. Verma, “Challenges and Limitation Analysis of an IoT Dependent System for Deployment in Smart Healthcare Using Communication Standards Features”, Journal of Sensor, vol. 23, issue 1, pp. 1-25, 2023.
34. L. Khelladi, D. Djenouri, M. Rossi, and N. Badache, “Efficient on-demand multi-node charging techniques for wireless sensor networks,” Computer Communications, vol. 101, pp. 44–56, 2017.
35. A. Tomar, L. Muduli, and P. K. Jana, “An efficient scheduling scheme for on-demand mobile charging in wireless rechargeable sensor networks,” Pervasive and Mobile Computing, p. 101074, 2019.
36. S. Upadhyay, SK Sharma & A. Upadhyay, “Speaker Identification and Verification Using Different Model for Text-Dependent”, International Journal of Applied Engineering Research, Vol. 12, No. 08, pp. 1633-1638, 2017.
37. J. Zhu, Y. Feng, M. Liu, G. Chen, and Y. Huang, “Adaptive online mobile charging for node failure avoidance in wireless rechargeable sensor networks,” Computer Communications, vol. 126, pp. 28–37, 2018.

38. C. Lin, S. Wei, J. Deng, M. S. Obaidat, H. Song, L. Wang, and G. Wu, “Gtccs: A game theoretical collaborative charging scheduling for on-demand charging architecture,” IEEE Transactions on Vehicular Technology, vol. 67, no. 12, pp. 12 124–12 136, 2018.
39. S. Upadhyay, M. Kumar, A. Upadhyay & K Z Gafoor, “Smart Healthcare Solution for Future Development using Speech Feature Extraction Integration Approach with IoT and Blockchain”, Journal of Sensors, vol. 2022 pp. 1-13, 2022.
40. K. E. Muller and B. A. Fetterman, Regression and ANOVA: an integrated approach using SAS software. SAS Institute, 2002.